



Communication

Two-dimensional TiO₂ (001) nanosheets as an effective photo-assisted recyclable sensor for the electrochemical detection of bisphenol ASujuan Hu^{a,b}, Yingjian Yu^c, Yu Guan^a, Yanhuan Li^a, Baoling Wang^{a,d}, Mingshan Zhu^{b,*}^a School of Chemistry and Chemical Engineering, Kunming University, Kunming 650214, China^b School of Environment, Jinan University, Guangzhou 510632, China^c Department of Physics Science and Technology, Kunming University, Kunming 650214, China^d Yunnan Engineering Technology Research Center for Plastic Films, Kunming University, Kunming 650214, China

ARTICLE INFO

Article history:

Received 4 July 2020

Received in revised form 28 July 2020

Accepted 11 August 2020

Available online 4 September 2020

Keywords:

TiO₂ (001) nanosheets

Bisphenol A

Electrochemical detection

Recyclable

Photo-assisted

ABSTRACT

Electrochemical detection is an efficient method for the detection of Bisphenol A (BPA). Herein, a sensitive photo-electrochemical sensor based on two-dimensional (2D) TiO₂ (001) nanosheets was fabricated and then used for BPA electrochemical detection. Upon light irradiation, the 2D TiO₂ (001) nanosheets electrode provided a lower detection limit of BPA detection compared with an ambient electrochemical determination. The low detection limit is ~5.37 nmol/L (S/N = 3). Furthermore, profiting from the photoelectric characteristics, the 2D TiO₂ (001) nanosheets electrode exhibits a nice regeneration property. After 45 min of light irradiation, the electrochemical signal was regenerated from 14.7% to 82.9% of the original signal at the 6th cycle. This is attributed to the non-selective [•]OH mediation produced by the 2D TiO₂ (001) nanosheets mineralizing anodic polymeric products and resuming surface reactive sites. This investigation indicates that photo-assistance is an efficient method to improve the electrochemical sensor for detecting BPA in water environments.

© 2020 Chinese Chemical Society and Institute of Materia Medica, Chinese Academy of Medical Sciences. Published by Elsevier B.V. All rights reserved.

Bisphenol A (BPA) is an environmental endocrine disruptor. It has an estrogenic effect that can mimic and interfere with endogenous estrogens and adversely affects the endocrine system, nervous system, immune system, and can even be teratogenic and carcinogenic [1,2]. Electrochemical detection is an efficient method for detecting the organic pollutant because of its simple sample preparation, fast response, high sensitivity, and easy operation [1–3]. However, during the electrochemical oxidation process of BPA, non-conductive polymer films are easily formed and adsorbed on the surface of the electrode, inactivating the electrode and affecting the sensitivity of BPA detection [4]. Therefore, eliminating the electrode surface non-conductive polymer and regenerating the fouling electrode is of great interest in developing reliable BPA monitoring [5,6].

Photochemical oxidation based on semiconductors can efficiently remove these surface contaminants by strong oxidizing species produced from the photo-excitation of a semiconductor [7–9]. TiO₂ is a typical semiconductor for practical applications because of its stable physical and chemical properties, low-cost, and nontoxicity [10–12]. Additionally, the potential of the valence

band (VB) of TiO₂ is greater than 1.99 eV, enabling it to produce holes and directly oxidize OH⁻ to [•]OH. [•]OH has a strong oxidizing ability. It can react with most organic pollutants and non-selectively oxidize them into CO₂, H₂O, or mineral salts. However, the utilization of holes is still limited as a consequence of the inherently high combination rate of photogenerated carriers of TiO₂ [13].

Two-dimensional (2D) TiO₂ with a largely exposed (001) single plane can provide rich surface atoms and large specific surface area for catalysis. Moreover, the migration length from the interior to the surface is reduced for photo-generated carriers because of the short thickness of the third dimension. Therefore, the recombination rate of the carriers is largely reduced. Herein, 2D TiO₂ (001) nanosheets were adopted for the detection of BPA in an aquatic environment. Under light irradiation, the 2D TiO₂ (001) nanosheets electrode produces abundant reactive oxygen species ([•]OH) with strong oxidation properties that can directly photodegrade the non-conductive polymer and realize the self-cleaning of the anode. The density functional theory (DFT) calculations show that the interfacial charge-transfer (ICT) transitions between the TiO₂ (001) and the BPA molecule under the light irradiation. The experimental and theoretical results suggest that the 2D TiO₂ (001) nanosheets electrode not only achieved a wide range detection of BPA, but also realized regeneration under simulated solar light irradiation.

* Corresponding author.

E-mail address: zhumingshan@jnu.edu.cn (M. Zhu).

The 2D TiO₂ (001) nanosheets were prepared by a solvothermal method [14]. The details of the characterizations of X-ray diffraction (XRD), scanning electron microscopy (SEM), transmission electron microscopy (TEM), UV/vis diffuse reflectance spectra (DRS) and X-ray photoelectron spectroscopy (XPS) and experimental sections are provided in Figs. S1 and S2 and corresponding discussions (Supporting information).

Generally, the differential pulse voltammetry (DPV) technique is a more efficient method to determine trace amounts BPA than the cyclic voltammetry (CV) technique because the non-Faradaic current produced by the CV technique can be eliminated by the intensive current signals of DPV [15–17]. Figs. 1A and C show DPV curves of the 2D TiO₂ (001) nanosheets electrode containing various concentrations of BPA with and without light irradiation, respectively. The oxidation peak currents were linearly proportional to the BPA concentration with a high correlation coefficient of > 0.98 (Figs. 1B and D). No oxidation peak appeared without the addition of BPA (Fig. S3 in Supporting information). Besides, under light irradiation, the 2D TiO₂ (001) nanosheets electrode exhibited a higher analytical signal and sensitivity for BPA (detection limit of ~5.37 nmol/L, S/N = 3) than that without light irradiation (detection limit of ~16.33 nmol/L, S/N = 3).

Although a sensitive detection result was achieved by using an electrochemical electrode, polymeric products were easily produced *in situ* on the electrode for most of the organic pollutant detection because of their reactivity and spontaneity. Not unexpectedly, the intensity of the anodic oxidation peak current of DPV gradually decreased for BPA detection within the 5-run cyclic test, and approximately 78% decrement after the 5-run cyclic measurement (Fig. S4 in Supporting information). Besides, the potential of the oxidation peak (~0.58 V vs. SCE) was increasingly positively shifted (Fig. S4). These results suggest that the severe fouling occurred on the surface of the electrode and the electron transfer resistance was increased.

For relieving the rapid decay of ability caused by electrode contamination and restoring electrode performance, the photochemical regenerated method was adopted. The fouling electrode (after the 5-run cyclic DPV measurement) was placed in deionized water with continued stirring for 15 min under the xenon lamp.

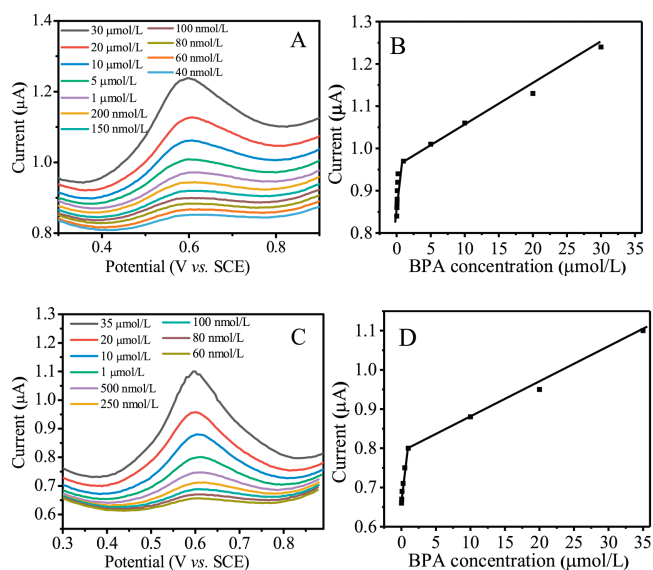


Fig. 1. The DPV responses of the 2D TiO₂ (001) nanosheets electrode with (A) and without (C) light irradiation; the corresponding plots of anodic oxidation photocurrent densities vs. the concentration of BPA (B) and (D). Measuring conditions: solution (0.1 mol/L PBS + 0.1 mol/L KCl solution + different concentrations of BPA, pH 7.0), scan rate (100 mV/S), potential range (0.3–0.9 V vs. SCE).

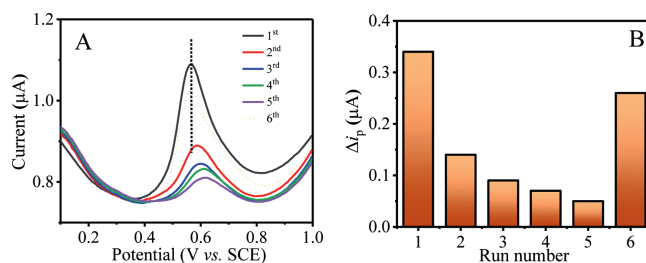
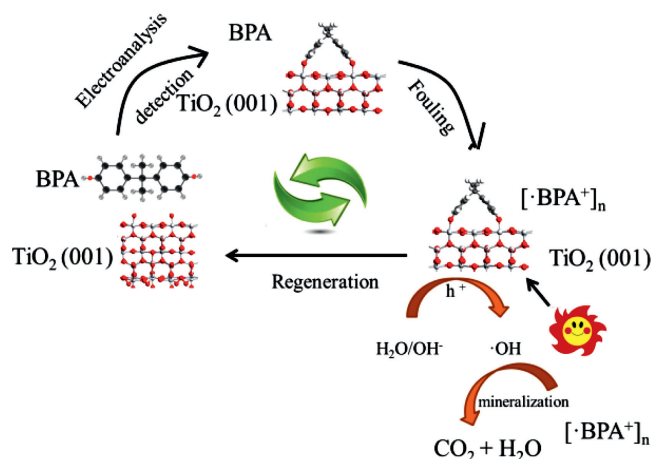


Fig. 2. (A) DPV responses of the 2D TiO₂ (001) nanosheets electrode (curves 1–5 are continuous test and curve 6 is the regenerated after light irradiation 45 min). (B) The corresponding peak intensity (ΔI_p) of DPV vs. cycle number, measuring conditions: Solution (0.1 mol/L PBS + 0.1 mol/L KCl solution + 10 μ mol BPA, pH 7.0), scan rate (100 mV/s), potential range (0.0–1.0 V vs. SCE).

Then, it was found that the oxidation peak current intensity of the 6th-run test was obviously improved compared to that of the 5th-run test. The decrement of oxidation peak current intensity decreased from 78% (5th-run) to 48% (6th-run). Then, the potential of oxidation peak returned to the original position (Figs. S5A and B in Supporting information). With an increase in irradiation time, the recovery of the oxidation peak current intensity improved. The decrement decreased to 39.1% and 18.1% after it was exposed to UV irradiation for 30 min and 45 min, respectively (Fig. 2 and Fig. S5 in Supporting information). These results demonstrate that electrode contamination can be greatly removed by 2D TiO₂ (001) nanosheets under light irradiation and that the electrode achieved regeneration. The specificity and reliability of the electrode were significant for BPA detection. Therefore, interfering tests with added structural analogues Bisphenol AF (BPAF) or Bisphenol D (BPD) are executed for BPA detection, as shown in Fig. S6 (Supporting information). The 2D TiO₂ (001) nanosheets electrode can be accurately detected without being affected by BPAF or BPD.

The nice photochemical regenerated property of the 2D TiO₂ (001) nanosheets electrode was mainly due to the non-selective \cdot OH mediation produced by the 2D TiO₂ (001) nanosheets electrode that could mineralize polymeric products and resume surface reactive sites. Holes produced by the 2D TiO₂ (001) nanosheets have strong oxidation ability and can directly activate H₂O/OH⁻ to \cdot OH [18,19]. \cdot OH can oxidize the polymeric products during BPA electrochemical detection, as shown in Scheme 1. Besides, the large portion of exposed (001) facet of TiO₂ effectively shortens the migration length of carriers from the interior to the surface, which inhibits photogenerated carriers recombination and improves the number of holes for \cdot OH. To verify this,



Scheme 1. Regeneration mechanisms of the 2D TiO₂ (001) nanosheets electrode-based electrochemical detector for cyclic BPA detecting.

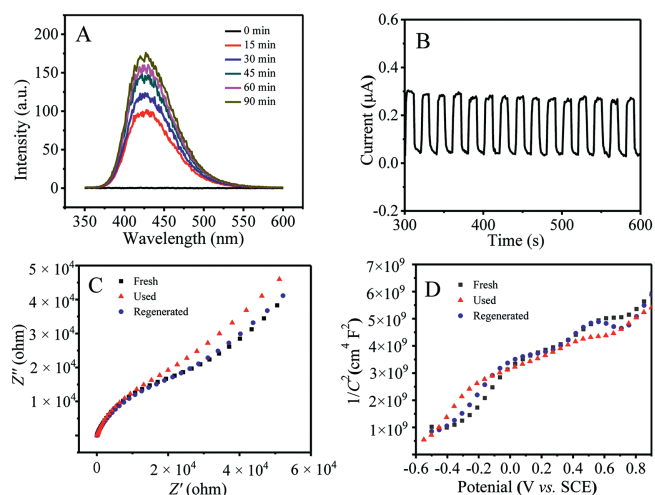


Fig. 3. PL spectra (A), photocurrent (B), EIS (C) and Mott-Schottky curves (D) of the 2D TiO₂ (001) nanosheets electrode. PL measuring conditions: terephthalic acid 0.014 g, NaOH 3 mmol/L, sample 0.1 g, 500 W Xe lamp, $\lambda < 420$ nm, stirring rate 500 rpm, excitation wavelength 315 nm. Photocurrent measuring conditions: solution (0.1 mol/L PBS + 0.1 mol/L KCl solution + 10 μ mol BPA, pH 7.0), 0.3 V of applied potential. EIS measuring conditions: solution (0.1 mol/L PBS + 0.1 mol/L KCl solution + 10 μ mol BPA, pH 7.0), voltage amplitude 5.0 mV, frequency range 10 kHz to 0.1 Hz and no bias. Mott-Schottky measuring conditions: solution (0.1 mol/L KCl + 0.1 mol/L PBS, pH 7.0), frequency (10³ Hz).

photoluminescence (PL) technology was adopted to detect the \cdot OH that was produced by the 2D TiO₂ (001) nanosheets, as exhibited in Fig. 3A. With the increase of illumination time, the PL intensity increased. Abundant nonselective high-activity \cdot OH can be produced under light irradiation of the 2D TiO₂ (001) nanosheets. Then, a transient photocurrent was adopted to investigate the charge separation property of the 2D TiO₂ (001) nanosheets electrode, as shown in Fig. 3B. A strong photo-response property and well charge separation efficiency can be obtained on the 2D TiO₂ (001) nanosheets electrode [20–23]. Following this, electrochemical impedance spectroscopies (EIS) were executed and the Mott-Schottky measurement was taken to verify the intrinsic characteristic of the 2D TiO₂ (001) nanosheets electrode after regeneration, as shown in Figs. 3C and D [24,25]. After the 10th-run cycle DPV test, the 2D TiO₂ (001) nanosheets electrode exhibited a large deviation with the fresh sample. However, after being illuminated for 45 min by a xenon lamp, the curves were close to that of the fresh sample. Fig. S7 (Supporting information) shows CVs of 10 μ mol/L BPA at different scan rates on the 2D TiO₂ (001) nanosheets electrode. The anodic photocurrent density increased linearly, the regression equations are $I_{pa} = 0.0509v + 2.51$ ($R^2 = 0.985$, without xenon lamp illumination) and $I_{pa} = 0.111v + 7.29$ ($R^2 = 0.993$, with xenon lamp illumination), indicating the electron transfer for BPA detection is a *quasi*-reversible and adsorption controlled process.

To further prove the ICT transitions between the TiO₂ (001) and the BPA molecule, DFT calculations of the TiO₂ (001)-BPA model was investigated, as shown in Fig. S8 (Supporting information). In this optimized configuration, the BPA molecule was adsorbed on the TiO₂ (001) surface by two Ti-O-C linkers, and the calculated adsorption energy was -23.27 eV (~ -23.02 kcal/mol), indicating a strong binding between the TiO₂ (001) surface and the BPA molecule. Figs. S8B and C presents the spatial distributions of the highest occupied molecule orbital (HOMO) and the lowest unoccupied molecule orbital (LUMO) of the complex. The HOMO is distributed at the interface and the LUMO is predominantly distributed in the TiO₂ substrate. This result indicates the existence of ICT transitions between the TiO₂ (001) and the BPA molecule under light irradiation [26–28].

The practical application of the 2D TiO₂ (001) nanosheets electrode as a photoelectrochemical (PEC) sensor for detecting BPA is carried out in various real water samples (Table S1 in Supporting information). However, the BPA concentration is too small to be directly detected in these real water samples. Therefore, standard addition was taken as the method for improving detection accuracy and recovery efficiency. The recoveries of BPA ranged from 97.18% to 102.1% for spiked lake water and 95.63%–102.2% for spiked tap water, respectively. Moreover, the relative standard deviation (RSD) was less than 5.5% for 3 successive measurements, suggesting that the present 2D TiO₂ (001) nanosheets electrode has suitable accuracy and can be applied to evaluate the concentration of BPA in real water.

In summary, a renewable 2D TiO₂ (001) nanosheets electrode sensor was fabricated and implemented to detect BPA in real water samples. With the help of photo-assistance, non-selective \cdot OH mediation produced by the 2D TiO₂ (001) nanosheets electrode mineralized polymeric products and resumed surface reactive sites, leading to the regeneration of electrode for BPA detection. Besides, the DFT calculations show the ICT transitions between the TiO₂ (001) and the BPA molecule under light irradiation. These results suggest that photo-assistance is an efficient method to improve the electrochemical sensor for detecting BPA in water environments.

Declaration of competing interest

The authors report no declarations of interest.

Acknowledgments

This study was supported by the Applied Basic Research Programs of Yunnan Science and Technology Department (No. 2017FD085), the Program of Introducing Talents of Kunming University (Nos. YJL16003 and YJL18008), National Nature Science Foundation of China (No. 61904073), Science Foundation of Yunnan Provincial Education Department (No. 2018JS392), Projects of Science and Technology Plans of Kunming (No. 2019-1-C-2531800002189), “Thousand Talents Program” of Yunnan Province for Young Talents, and Spring City Plan-Special Program for Young Talents.

Appendix A. Supplementary data

Supplementary material related to this article can be found, in the online version, at doi:<https://doi.org/10.1016/j.ccl.2020.08.021>.

References

- [1] T.D. Vu, P.K. Duy, H.T. Bui, S.H. Han, H. Chuang, *Sens. Actuators B* 281 (2019) 320–325.
- [2] J. Li, Y. Li, Z. Xiong, G. Yao, B. Lai, *Chin. Chem. Lett.* 30 (2019) 2139–2146.
- [3] Z. Fan, L. Fan, S. Shuang, C. Dong, *Talanta* 189 (2018) 16–23.
- [4] R. Liu, H. Zhao, X. Zhao, et al., *Environ. Sci. Technol.* 52 (2018) 9992–10002.
- [5] B.L. Hanssen, S. Siraj, D.K.Y. Wong, *Rev. Anal. Chem.* 35 (2016) 1–28.
- [6] A. Ghanam, A.A. Lahcen, A. Amine, *J. Electroanal. Chem.* 789 (2017) 58–66.
- [7] V. Silva-Castro, J.C. Durán-Álvarez, J. Mateos-Santiago, et al., *Mater. Sci. Semicond. Process.* 72 (2017) 115–121.
- [8] Y. Si, A.Y. Zhang, C. Liu, D.N. Pei, H.Q. Yu, *Water Res.* 157 (2019) 30–39.
- [9] L.A. Goulart, S.A. Alves, L.H. Mascaró, *J. Electroanal. Chem.* 839 (2019) 123–133.
- [10] S. Hu, B. Wang, M. Zhu, et al., *Appl. Surf. Sci.* 403 (2017) 126–132.
- [11] S. Hu, B. Wang, H. Ju, et al., *J. Taiwan Inst. Chem. Eng.* 80 (2017) 533–539.
- [12] W. Wang, F. Liu, B. Wang, Y. Wang, *Chin. Chem. Lett.* 30 (2019) 1261–1265.
- [13] Z. Yan, W. Wang, L. Du, et al., *Appl. Catal. B* 275 (2020) 119151.
- [14] H.G. Yang, G. Liu, S.Z. Qiao, et al., *J. Am. Chem. Soc.* 131 (2009) 4078–4083.
- [15] J. Wang, B. Yang, S. Li, et al., *J. Colloid Interface Sci.* 506 (2017) 329–337.
- [16] J. Wang, K. Zhang, H. Xu, et al., *Sens. Actuators B* 276 (2018) 322–330.
- [17] B. Yang, D. Bin, K. Zhang, Y. Du, T. Majima, *J. Colloid Interface Sci.* 512 (2018) 446–454.
- [18] J. Chen, Z. He, Y. Ji, et al., *Appl. Catal. B* 257 (2019) 117912.

- [19] T.M. Khedr, S.M. El-Sheikh, A.A. Ismail, D.W. Bahnemann, *Opt. Mater.* 88 (2019) 117–127.
- [20] H. Zhang, J. He, C. Zhai, M. Zhu, *Chin. Chem. Lett.* 30 (2019) 2338–2342.
- [21] L. Cai, Y. Du, X. Guan, S. Shen, *Chin. Chem. Lett.* 30 (2019) 2363–2367.
- [22] S. Feng, P. Yan, L. Xu, J. Xia, H. Li, *Chin. Chem. Lett.* 29 (2018) 1629–1632.
- [23] C. Zhao, H. Tang, W. Liu, et al., *ChemCatChem* 11 (2019) 6310–6315.
- [24] H. Xu, H. Shang, C. Wang, et al., *Appl. Catal. B* 265 (2020) 118605.
- [25] F. Gao, Y. Zhang, P. Song, et al., *J. Mater. Chem. A* 7 (2019) 7891–7896.
- [26] J.I. Fujisawa, S. Matsumura, M. Hanaya, *ChemistrySelect* 2 (2017) 6097–6099.
- [27] J.I. Fujisawa, S. Matsumura, M. Hanaya, *Chem. Phys. Lett.* 657 (2016) 172–176.
- [28] J.I. Fujisawa, S. Matsumura, M. Hanaya, *ChemistrySelect* 1 (2016) 5590–5593.